Illumination Level Independence in the Dynamic Laser Speckle Analysis

Fernando Pujaico Rivera, Roberto Alves Braga Jr.

University Federal of Lavras, Lavras, Brazil

Abstract

In this article we show an analysis of how the frequency band, of the speckle signal, influence in the light independence of the speckle index value in a dynamic laser speckle analysis. Specifically, will be studied as It is influenced the temporal speckle deviation index by the use of 3 different frequency bands of the speckle signal. Finally, It is shown as signals with high frequency values return values with more illumination level independence.

Keywords: Biospeckle laser, Biospeckle index, Biospeckle signal, Biological activity, Dynamic speckle

1. Introduction

Dynamic laser speckle is a phenomenon that is used to monitor changes in illuminated samples, and it can be measured by multiple indexes [1]. The indexes are associated to the level of changes and could be expressed by numerical and or graphical outcomes that can be affected by filtering action during the image processing [2]. As an example, we have the AVD [3] and IM [4] indexes, that filter the information present in the history of the speckle images like a first order high pass filter with a cut-off in the middle of the normalized frequency band. For this reason, it is important to analyze how the chosen frequency band alters the result of selected index. By other side, there is still a limitation to

[1]201518201@posgrad.ufla.br
[2]robertobraga@deg.ufla.br

make speckle analysis in the presence of in-homogeneity of illumination, because the most of biospeckle indexes are influenced in their values by the use of a illumination level [5]. The illumination level can vary regarding the profile of the sample, such as an apple [6] or a very irregular surface present in a kefir [7]. It can also vary in accordance with the moisture present in the seed [8] due to the penetration of the light in the sample, or even when the color of the sample vary such as in the interface of cancer and normal tissues [9]. And that is the reason to a continuous search for an adequate index, despite the fact there are many of them present in literature [1], but still without a solution to the independence of light intensity. The movement toward the portable equipment [10], reinforce the need to search the methods and its relation with the illumination. Thus, the present work aimed to establish a relation between the frequency band used and the speckle index; particularly in the dependence of the temporal speckle deviation matrix [11] with the illumination level.

2. System description

2.1. Data packages of drying ink

Fig. 1 shows the system setup of the ink sample test during drying where a red laser was pointed to a layer of drying ink monitored by a digital camera; the images are collected receiving two different illumination levels, because of the neutral density lens covering partially the laser beam [5]. The images were placed in data packages and are sampled with a time rate acquisition of $F_s = 12.5$ hertz, being collected $N = 400$ images by package. In total were collected 11 packages (with the two different illumination levels each one) at the minutes 0, 10, 20, 30, 40, 50, 60, 75,105,120 and 150 of drying process. In each image of the packages were selected two regions, of 250×200 pixels, corresponding to the regions with two different illumination levels, as shown with red lines in the Fig. 2; thus, in the right side of the Fig. 2 we have the portion of image that was altered by the neutral density lens.

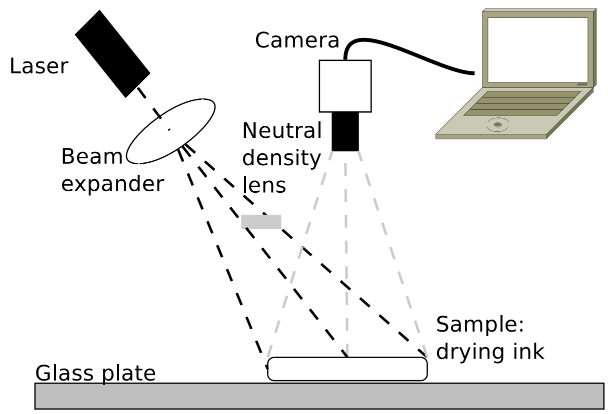

Figure 1: Experimental configuration of dynamic laser speckle formation monitored by digital system with the levels of illumination over a layer of drying ink.

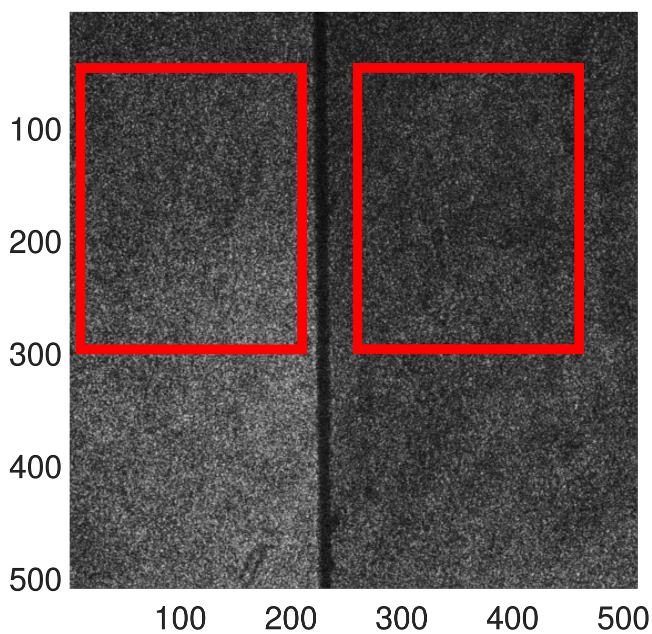

Figure 2: Selected regions and light intensity distribution in the ink drying test.

2.2. Data packages of a steady state paper

The test over a steady state paper has a similar configuration that seen in the Fig. 1 with the the absence of the neutral density lens. The phenomenon observed was the noise associated to the experimental configuration linked to the camera, to the resolution of the images and also the mechanical noise, and it was collected one data package sampled with a frequency of $F_s = 10$ hertz, being collected in total $N = 129$ images of 640×480 pixels. The Fig. 3 represents with a color bar the result of calculus the temporal speckle mean matrix (μ) according the Eq. (2) showed in the Sec. 3.2; thus, it is easy to see how the illumination level of laser over the paper has an elliptical form being highest close to the top of the image.

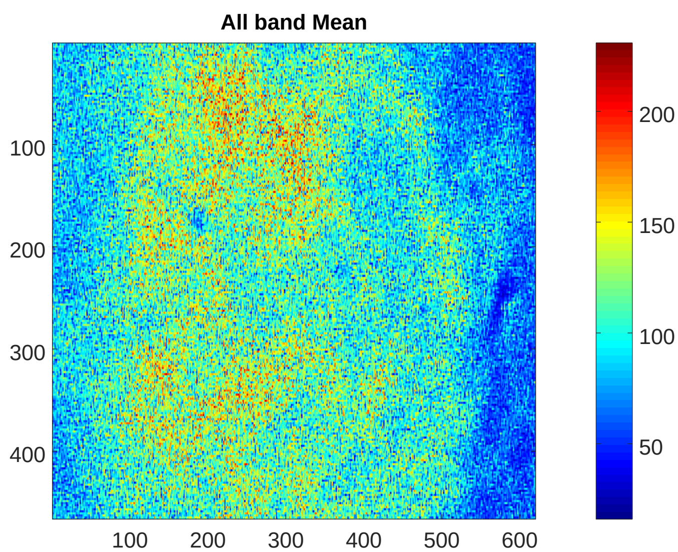

Figure 3: Light intensity distribution in the paper piece test with highest illumination presented by red pixels and lowest by blue pixels.

3. Numerical analysis

3.1. Data package filtering in three frequency band

Each data package or sub package (P_T) went through of a filter bank with 4 outputs having each one a different type of processing, the first output is trivial because it lets to pass the information freely, this package is called of P_T, whilst the other 3 outcomes return signals filtered by a frequency band; thus, we have the band between $[0, \frac{1}{3}]\frac{F_s}{2}$ (low frequencies), the band between $[\frac{1}{3}, \frac{2}{3}]\frac{F_s}{2}$ (intermediate frequencies) and the band between $[\frac{2}{3}, 1]\frac{F_s}{2}$ (high frequencies); obtaining at end, the packages P_X, P_Y and P_Z, respectively; as can be seen in the Fig. 4. The filtered packages of images were carried out using cascades of two low-pass Finite Impulse Response (FIR) filters of order 32, so that the sum of signals $P_X + P_Y + P_Z = P_T$.

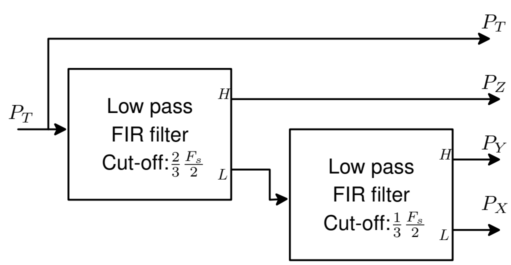

Figure 4: Filtering of data packages.

3.2. Temporal speckle deviation matrix

The temporal speckle deviation matrix (σ) [11] used to compare the results was obtained from the N images of a data package. We designate to each image, in the package P, as $\mathbf{I}_k$, $1 \leq k \leq N$, being k an integer; thus, to get the value σ, it is necessary to get the matrix σ as seen in the Equation 1,

$$\sigma = \sqrt{\frac{1}{N}\sum_{k=1}^{N}(\mathbf{I}_k - \mu)^2}, \tag{1}$$

being that, the value μ can be calculated as,

$$\mu = \frac{1}{N}\sum_{k=1}^{N}\mathbf{I}_k, \tag{2}$$

Additionally, the temporal speckle deviation index can be defined as $\bar{\sigma} =< \sigma >$, the mean value of all elements in σ, being $< . >$ the mean spatial operator.

3.3. Datapack processing in the test of a drying ink

We have in the drying ink regions two levels of illumination; thus, we separated each package in two sub package (left and right), representing each one of the regions shown in the Fig. 2. These sub-packages were filtered, obtaining the packages P_T, P_X, P_Y and P_Z, that was used to obtain the temporal speckle

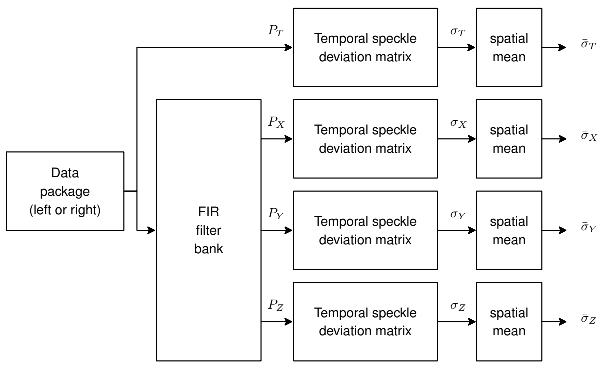

Figure 5: Filtering of data packages.

deviation matrix and the temporal speckle deviation indexes $\bar{\sigma}_T$, $\bar{\sigma}_X$, $\bar{\sigma}_Y$ and $\bar{\sigma}_Z$.

3.4. Statistical analysis of relation between the matrices σ and μ

We defined σ_i and μ_i as the values in the $i-th$ position in the σ and μ matrices, respectively; we also defined μ_p as any element value in μ. And we define the set $S_{\mu_p} = \{\sigma_i : \mu_i \equiv \mu_p; \forall i\}$ as the set of all σ_i values given that $\mu_i \equiv \mu_p$. Then, we obtained the vectors L_p, σ_p and e_p using all the μ_p values, according to:

- $L_p(\mu_p) = card\left(S_{\mu_p}\right)$, being $L_p(\mu_p)$ the number of elements in the set S_{μ_p} and $card(.)$ the cardinality function operator.

- $\sigma_p(\mu_p) = mean\left(S_{\mu_p}\right)$, being $\sigma_p(\mu_p)$ the mean value of elements in the set S_{μ_p} with $mean(.)$ representing the mean value function operator.

- $e_p(\mu_p) = std\left(S_{\mu_p}\right)$, being $_p(\mu_p)$ the standard deviation value of elements in the set S_{μ_p} with $std(.)$ representing the standard deviation function operator.

In practice only will be taken the vectors, values of μ_p with a $L_p(\mu_p) > 200$ samples, to establish a limit to consider a set of representative samples.

3.5. Datapack processing in the test of a steady state paper

In this test we have one data package that was filtered (6) obtaining the packages P_T, P_X, P_Y and P_Z, where the outcomes are the temporal speckle mean matrix and the temporal speckle deviation matrix, as can be seen in the Fig. 6.

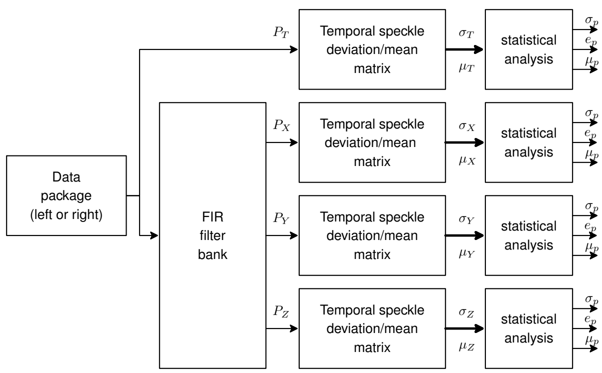

Figure 6: Filtering of data package in the steady paper obtaining the mean and the deviation outcomes.

4. Numerical results

4.1. Numerical results o the drying ink test

In the Fig. 7, we can see the result of processing the drying ink test under the dynamic laser speckle index (DLSI) in two areas with different level of illumination. The Fig. 7a represents the $\bar{\sigma}_T$ value in two light intensity levels, and it is done using the package P_T trough the time, with the complete frequency bands. The Fig. 7b represents the $\bar{\sigma}_X$ value in two light intensity levels, an it is done using the package P_X trough the time, with the frequency band between 0 and $\frac{1}{3}\frac{F_s}{2}$Hz. The Fig. 7c represents the $\bar{\sigma}_Y$ value in two light intensity levels, and it is done using the package P_Y trough the time, with the frequency band between $\frac{1}{3}\frac{F_s}{2}$ and $\frac{2}{3}\frac{F_s}{2}$ Hz. And the Fig. 7d represent the $\bar{\sigma}_Z$ value in two light intensity levels, and it is done using the package P_Z trough the time, with the frequency band between $\frac{2}{3}\frac{F_s}{2}$ and $\frac{F_s}{2}$ Hz. As can be seen, when we analyzed the

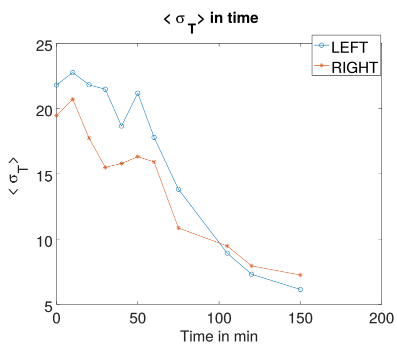

(a) $\bar{\sigma}_T$ value through the time.

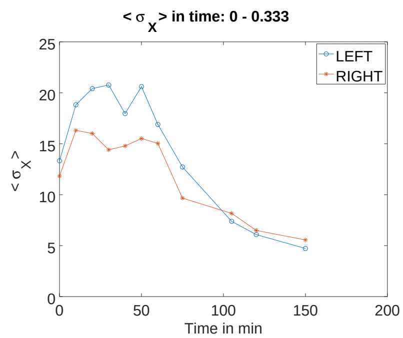

(b) $\bar{\sigma}_X$ value through the time.

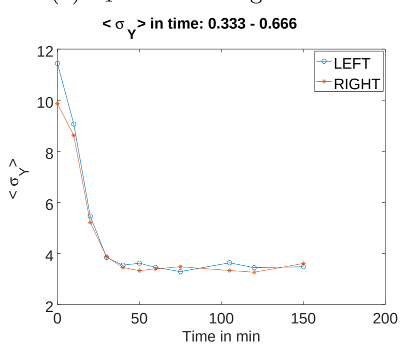

(c) $\bar{\sigma}_Y$ value through the time.

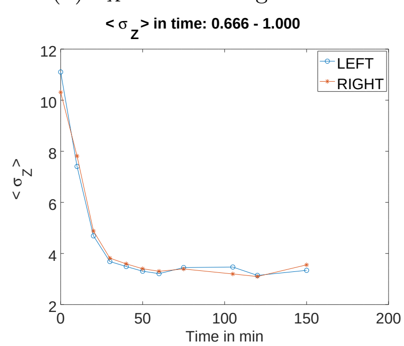

(d) $\bar{\sigma}_Z$ value through the time.

Figure 7: Numerical results in the ink drying test.

index over the complete frequency band (Fig. 7a), we had different results to both illuminations levels, being high in the left side,that is the side with most illumination. This indicates a positive influence of illumination level in the index value. By other side, if we observe the Figures 7b, 7c and 7d we can see how the index values from different illuminations was similar to the frequency level, being greatest similarity in the frequency band between $\frac{2}{3}\frac{F_s}{2}$ and $\frac{F_s}{2}$ Hz. Thus the similarity is limited by the sampling rate used.

Finally, it is important to highlight that in the drying ink test, the information from the dynamic laser speckle is linked to high frequencies in the beginning of the drying process and speckle signals with low frequencies at end, being gradual the transition until reach the lowest level of signal with only the noise of test. In Figure 7 $(c-d)$ one can see that after 50 minutes there is a transition of state with the stabilization of the DLSI. Thus, after this point, one has only the inner noise of the system influencing the DLSI.

This indicates that the comparisons of index illumination independence only should be made between the first minutes because out this range we will be using high contribution of the noise as outcome.

4.2. Numerical results of a steady paper under laser light

In the Fig. 8 we can see the result of data processing from the steady paper under dynamic laser speckle phenomenon considering an homogeneous illumination and using the standard deviation σ as a dynamic laser speckle index (DLSI). Fig. 8a represents the σ_T matrix with the complete frequency band, while Fig. 8b represents the σ_X matrix with the frequency band between 0 and $\frac{1}{3}\frac{F_s}{2}$Hz. Fig. 8c represents the σ_Y matrix with the frequency band between $\frac{1}{3}\frac{F_s}{2}$ and $\frac{2}{3}\frac{F_s}{2}$ Hz, and Fig. 8d represents the σ_Z matrix with the frequency band between $\frac{2}{3}\frac{F_s}{2}$ and $\frac{F_s}{2}$ Hz.

In Figure 9 we present the relation between an average value of σ_p, in the σ matrix, with a value μ_p (mean value representing the illumination level) of the μ matrix, to all frequency bands, the value μ_p is related to the illumination level in the surface of the sample [11] and the color or material of sample. Thus, when we choose μ_p as reference in a homogeneous sample, in true we choose indirectly the illumination level in the surface. Therefore, Fig. 9 shows the variables σ_p, e_p and L_p in function of μ_p, to the case of the complete frequency band (9a), the inferior third of the frequency band (9b), the middle third of the frequency band (9c) and the superior third of the frequency band (9d). It is import to note that e_p was plot as a relation of σ_p, this means $100\frac{e_p}{\sigma_p}\%$.

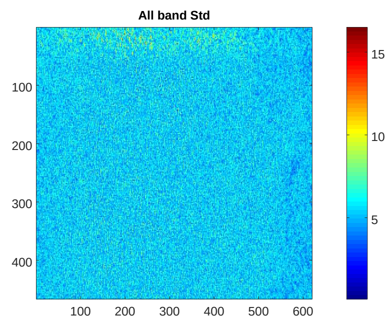

(a) σ_T matrix over the complete frequency band.

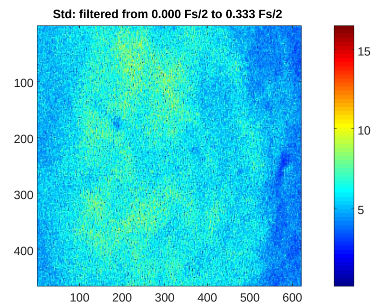

(b) σ_X matrix over the inferior third of the frequency band.

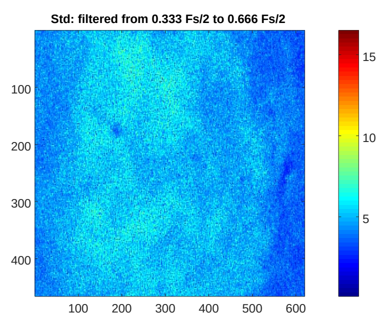

(c) σ_Y matrix over the middle third of the frequency band.

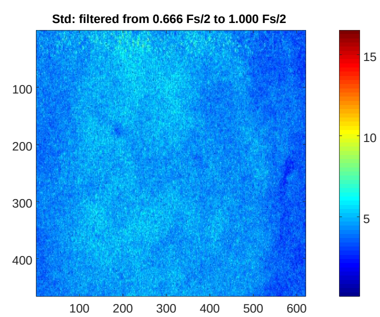

(d) σ_Z matrix over the superior third of the frequency band.

Figure 8: Temporal speckle deviation matrix of paper piece.

In Figure 9a, we observe the absence of tendency in the DLSI (σ) with respect to the intensity (μ), i.e. with the increase of the μ value the standard deviation (σ) does not increase or decrease. However, around that constant there is a spread of σ to each value of μ that creates an uncertainty in the outcome, and expressed by the error e. Figure 9a represents the outcome from the data without filtering, thus with all frequencies. And the data is the noise present in the processes of illumination and image acquiring because the sample is a steady paper without changes in the scatterers of the laser light. Nevertheless, when we filter the signal (images in time), we can observe a change in the σ with respect to the frequency range, unveiling the dependency of the DLSI to

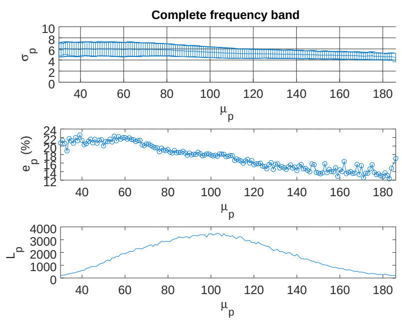

(a) Analysis in the complete frequency band.

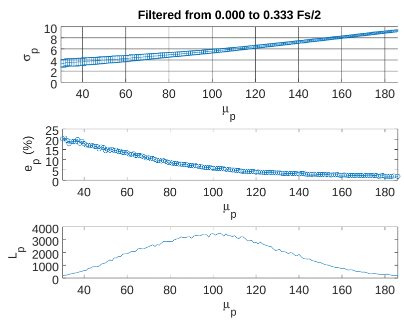

(b) Analysis in the inferior third of the frequency band.

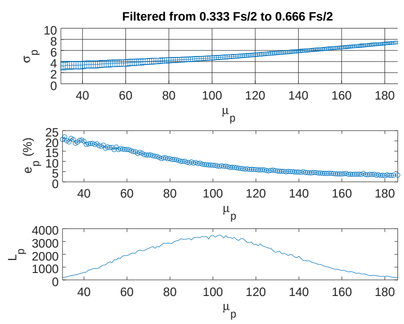

(c) Analysis in the middle third of the frequency band.

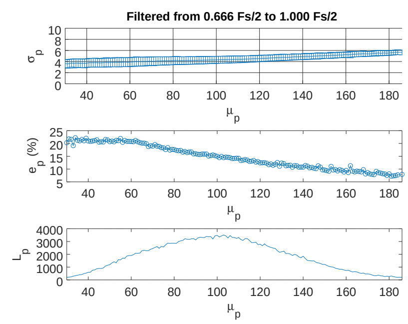

(d) Analysis in the superior third of the frequency band.

Figure 9: Relation between the standard deviation value and the illumination level in a steady paper under laser illumination.

the level of illumination and its relation to the frequency. In Figure 9b, in the inferior third of the frequency band, there is a tendency in the σ value with respect to the level of light. The DLSI changes its value with respect to the illumination level, where in low illumination level one had highest error, with the σ values spread around the mean value, and the error tending to zero when the level of light increased in some areas of the sample. The same behavior happened in the middle level of frequency band, and much less in the superior third of the frequency band, meaning that in the highest frequencies one had less influence of the level of light in the σ values. Since the σ DLSI does not filter the signal [2], it must be considered this situation during the DLSI usage, as one can compromise the outcome by the influence of the illumination of the sample in the results. Dynamic laser speckle indexes can offer other index options to circumvent that influence, for example, using the Absolute Value of the Differences DLSI and its variations [1].

5. Conclusion

In this work were presented comparisons between the values of the temporal speckle deviation index to three different frequency bands of the speckle signal and different illuminations levels, in a dynamic laser speckle analysis. The results showed that the influence of the illumination level in the DLSI index, like the temporal speckle deviation index, decreases with the use of signals with high frequency bands.

6. Acknowledgment

We wish to acknowledge the partial financial support for this study provided by the *CAPES* scholarship *PNPD* Program, *FAPEMIG* and *CNPQ*.

7. Bibliography

[1] R. A. Braga Júnior, F. Pujaico Rivera, J. Moreira, A practical guide to biospeckle laser analysis: theory and software, Ed. UFLA, 2016. URL `https://repositorio.ufla.br/handle/1/12119`

[2] F. P. Rivera, R. A. Braga, Selection of statistical indices in the biospeckle laser analysis regarding filtering actions, Optics Communications 394 (2017) 144 – 151. `doi:10.1016/j.optcom.2017.03.015`.

[3] R. Braga, C. Nobre, A. Costa, T. Sáfadi, F. da Costa, Evaluation of activity through dynamic laser speckle using the absolute value of the differences, Optics Communications 284 (2) (2011) 646650. `doi:10.1016/j.optcom.2010.09.064`.

[4] R. Arizaga, M. Trivi, H. Rabal, Speckle time evolution characterization by the co-occurrence matrix analysis, Optics Laser Technology 31 (2) (1999) 163 – 169. doi:10.1016/S0030-3992(99)00033-X.

[5] R. O. Reis, H. J. Rabal, R. A. Braga, Light intensity independence during dynamic laser speckle analysis, Optics Communications 366 (2016) 185 – 193. doi:10.1016/j.optcom.2015.12.062.

[6] A. Kurenda, A. Adamiak, A. Zdunek, Temperature effect on apple biospeckle activity evaluated with different indices, Postharvest Biology and Technology 67 (2012) 118–123.

[7] R. O. Viana, K. T. Magalhes-Guedes, R. A. Braga, D. R. Dias, R. F. Schwan, Fermentation process for production of apple-based kefir vinegar: microbiological, chemical and sensory analysis, Brazilian Journal of Microbiology 48 (3) (2017) 592 – 601. doi:10.1016/j.bjm.2016.11.006.

[8] R. R. Cardoso, A. G. Costa, C. M. B. Nobre, R. A. Braga, Frequency signature of water activity by biospeckle laser, Optics Communications 284 (8) (2011) 2131 – 2136. doi:10.1016/j.optcom.2011.01.003.

[9] R. Braga, R. Cardoso, P. Bezerra, F. Wouters, G. Sampaio, M. Varaschin, Biospeckle numerical values over spectral image maps of activity, Optics Communications 285 (2012) 553–561.

[10] R. Braga, Challenges to apply the biospeckle laser technique in the field, Chemical Engineering Transactions 58 (2017) 577–582.

[11] R. Nothdurft, G. Yao, Imaging obscured subsurface inhomogeneity using laser speckle, Optics Express 13 (25) (2005) 10034–10039. doi:10.1364/OPEX.13.010034.